



ISSN: 0067-2904

Preparation of PPy-WO₃ Nano-composite for Supercapacitor Applications

Firas J. Hameed^{*}, Isam M. Ibrahim

Department of physics, College of Science, University of Baghdad, Baghdad, Iraq

Received: 30/3/2020

Accepted: 17/6/2020

Abstract

In this work, polypyrrole (PPy) composites were chemically prepared by a chemical oxidation method. Also, Tungsten Trioxide (WO₃) nanoparticles were prepared and added in certain proportions to PPy. The structure properties were studied for the polypyrrole and tungsten trioxide separately before mixing them together. The X-ray diffraction (XRD) analysis revealed a hexagonal WO₃ and a triclinic PPy. It was observed that the nano-composite prepared by the addition of WO₃ with 10 and 20% volume ratios to PPy shows a triclinic phase with the presence of hexagons. The molecular structures of PPy, WO₃, and PPy-WO₃ nano composites were depicted by Fourier-transform infrared spectroscopy (FTIR) in the scope of 400–4000 cm⁻¹. The supercapacitors of PPy and PPy-WO₃ were examined by calculating the figure of merit of the electrode (PPy and PPy-WO₃) using cyclic voltammetry (CV), galvanostatic charge and discharge (GCD), and electrochemical impedance spectroscopy (EIS) techniques. It was found that the highest value of capacity (266.62 F/g) is obtained at 20% WO₃ ratio.

Keywords: Polypyrrole (PPy), Structural Properties, supercapacitor

تحضير قطب من مركب PPy-WO₃ لتطبيقات كهروكيميائية

فiras جاسم حميد^{*}، عصام محمد ابراهيم

قسم الفيزياء، كلية العلوم، جامعة بغداد، بغداد، العراق

الخلاصة:

في هذا البحث ، تم تحضير مركبات PPy كيميائياً بطريقة الأوكسدة الكيميائية ، بالإضافة إلى تحضير جسيمات نانوية WO₃ وأضيفت نسب معينة من WO₃ إلى PPy. تمت دراسة الخصائص التركيبية (XRD و FTIR) للمادتين بشكل منفصل ثم تم خلطهما معاً. حيث وجد ان حيود الأشعة السينية من WO₃ تكون سداسية و Ppy طور ثلاثي. وقد لوحظ عند إضافة (10 و 20% حجم) من WO₃ إلى Ppy يظهر تركيب المركب النانوي طور ثلاثي مع وجود السداسي. تم تصوير التركيب الجزيئي للمركبات النانوية Ppy و WO₃ و PPy-WO₃ بواسطة التحليل الطيفي بالأشعة تحت الحمراء فورير (FTIR) في نطاق (4000-400) سم⁻¹. تم فحص المكثفات الفائقة ل Ppy و PPy-WO₃ وذلك بواسطة (CV، GCD، EIS). وجد أن أكبر سعة تم الحصول عليها بنسبة 20% WO₃ حيث كانت السعة 266.62 (F / g).

1. Introduction

The conducting polymers (CPs) are suitable for favorable conditions to allow conducting the charge current of a simple electron by the polymer network in electrochemical procedures [1-3]. PPy is one of the most commonly used CPs considering its simplicity of blending, good conductivity, and

*Email: firasalhbole@gmail.com

environmental stability [4]. Bonding is a primary necessity for PPy's electrical effects. The electrical conductivity of PPy is likely to be upgraded through catalysis processes that lead to the joining of counters such as cations, inorganic anions, natural molecules, etc. [5]. The unique properties of CPs open up new potential outcomes of mechanical processes; for example, in recharging batteries or biochemical allergens. CPs can store the capacitance by the mechanism of accumulation/release of countercharges due to redox reactions arising under the electric field [6-10]. The introduction of electrostatic polymers remains the subject of extensive examination by researchers around the world. These conductive polymers have unique electrochemical properties in terms of the ability to rapidly discharging steroids and doping. The aim of this process could be to trap the charge in all volumes. Only few types of conductive polymers have the property of super-condensation, such a poly (PPy), poly (1, 5-diamino anthraquinone), and polyaniline (PANI). PPy is a specially oriented polymer due to its high conductivity, high storage capacity, environmental stability, and strong redox current [11-12]. Generally, capacitors are built using a set of parallel connection plates that are separated by an insulator. The capacitive charge of the opposite sign builds up when voltage is applied to the plates in series. These conventional capacitors have low (mF) power values, but the supercapacitors have the high capacities (F) [20]. This study aimed to prepare an electronic electrode, investigating its structural properties, and then measuring the figure of merit for super capacitor, such as GCD, EIS, CD, and impedance

2. Experimental Work

2.1 Synthesis of PPy Nanostructure

The combination of polypyrrole nanostructure was built up based on the methodology described by Yang [14]. The initial step was built up with complete scattering of 0.818 g of methyl orange in 60 mL distilled water. Under slow stirring of 80 rpm and submerging in an ice bath, 2.237g of ferric chloride was scattered at fluid arrangement of methyl orange with incorporation of 1 mL of pyrrole. The blend procured a blackish appearance and was kept under stirring for 24 hours. The precipitant was filtered and washed with ethanol and distilled water many times, then vacuum-dried for 60 minutes.

2.2 Synthesis of WO₃ Nanoparticles

For the preparation of WO₃ nanoparticles, 0.1 g of WO₃ was dissolved with 100 ml of distilled water and stirred for 10 min at a temperature of 60 °C. Drops of ammonium hydroxide (NH₄OH) were added until the pH was adjusted to 8. The mixture was filtered and washed with ethanol and distilled water many times, then vacuum-dried at 60 °C for 60 minutes. After that, the resulted material was placed in an oven at 400 °C for 1 hour to obtain a stable phase of tungsten oxide.

2.3 Preparation of PPy/WO₃ nanocomposite

An appropriate amount of WO₃ was dispersed in distilled water and added to PPy with volume ratios of 10%:90% and 20%:80% and subjected to ultrasonic waves for 1 hour to obtain a ready-to-use homogenous dispersion.

2.4 Preparation of the electrode

Nickel foam (1*1 cm²) substrate was used for the preparation of the PPy:WO₃ as an electrode. PPy:WO₃ nanocomposite with ratios of 10%:90% and 20%:80%, respectively, was deposited on nickel foam substrate, by using the drop casting method. The prepared sample (PPy:WO₃ / nickel foam) was placed in 1 ml of concentrated sulphuric acid (100% H₂SO₄) for testing the cyclic voltammetry (CV), galvanostatic charge–discharge examination (GCD), and electrochemical impedance spectroscopy (EIS). The mass of the electrode (PPy:WO₃) was 0.7mg. Figure 1 shows a schematic diagram of the prepared sample which was used as an electrode for the supercapacitor.

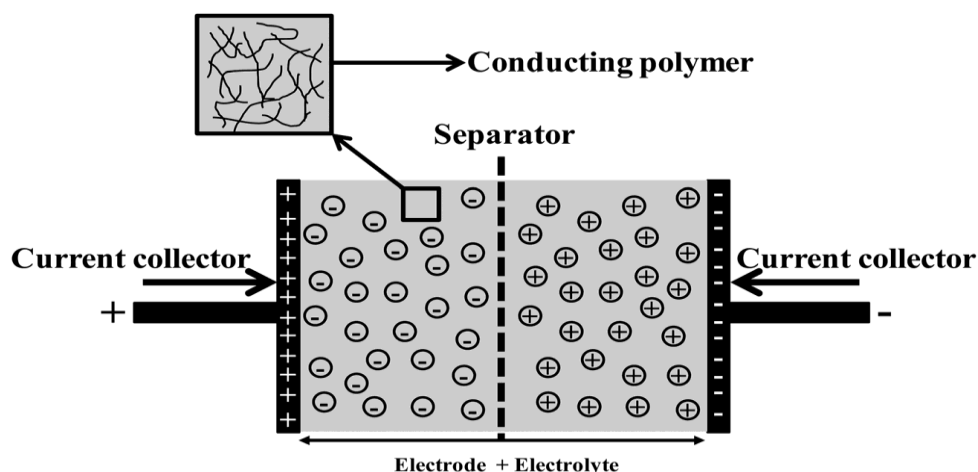
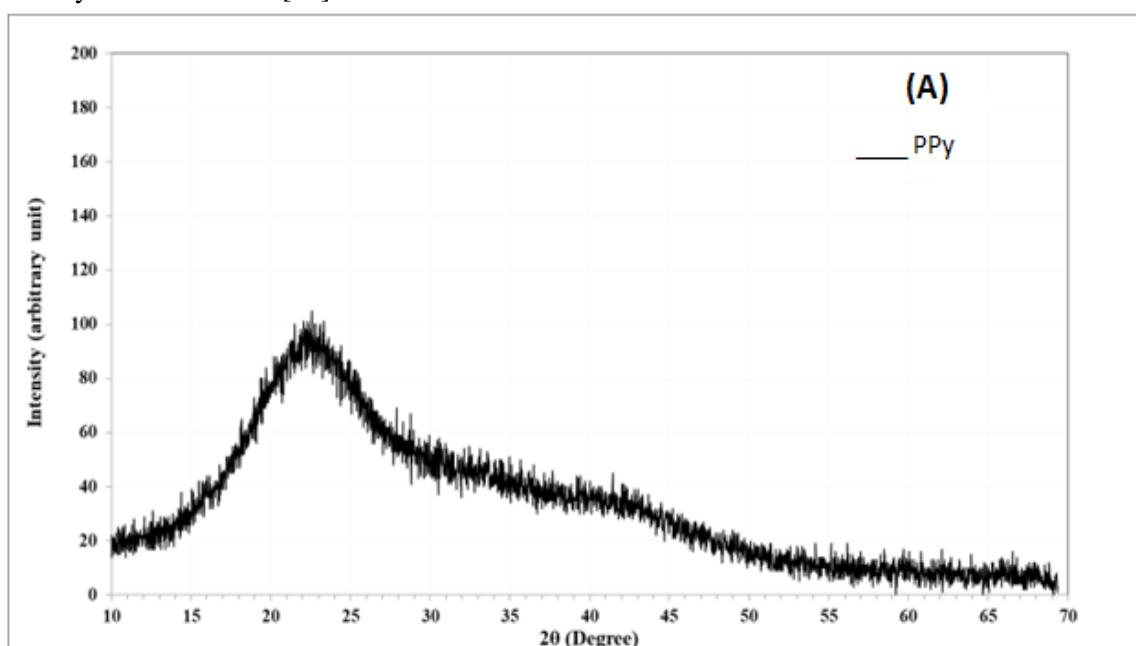


Figure 1- A schematic diagram of the electrochemical supercapacitor using a conductive polymer layer as the material for the electrodes

3. Results and Discussion

3.1 Analyzing X-ray diffraction

The structural analysis of PPy and the two concentrations of PPy–WO₃ hybrid nanocomposite were achieved by XRD. Figure 2(A) represents the XRD of PPy which indicates the wide diffraction peak at $2\theta = 17 - 28$, which characterized PPy for its one peak form arranged by substance oxidative polymerization strategy [15]. Figure 2(B) shows XRD results of PPy: WO₃ (90:10% and 80:20%) hybrid nanocomposites. It shows sharp and characterized peaks having the orientations of (100), (001), (200), (020), (002), (400), (040), (110), (120), (021), (201), (220), (202), (022), (401), (041), (111), (121), (221), (222), and (421) planes. The peaks are in close concurrence with the detailed Cod (crystallography open database) 1010618 and Cod 1004057. The expansive spike of diffraction of PPy is covered by the noble element appearances of WO₃ nanoparticles with enormous diffraction powers of (001), (020), (200), (120), and (111). From these results, it is concluded that PPy has a triclinic shape whereas WO₃ is hexagonal. Nonetheless, PPy-WO₃ nanocomposite appeared as a mix of triclinic and hexagonal shapes. In addition, it was observed that the WO₃ nanoparticles have significant effects on PPy, making a hybrid nanocomposite material with polycrystalline structure [16]. This observation proposes homogeneous scattering of the WO₃ nanoparticulates in the PPy network without any agglomeration by a specified percentage of WO₃. This result corresponds to that shown by an earlier work [17].



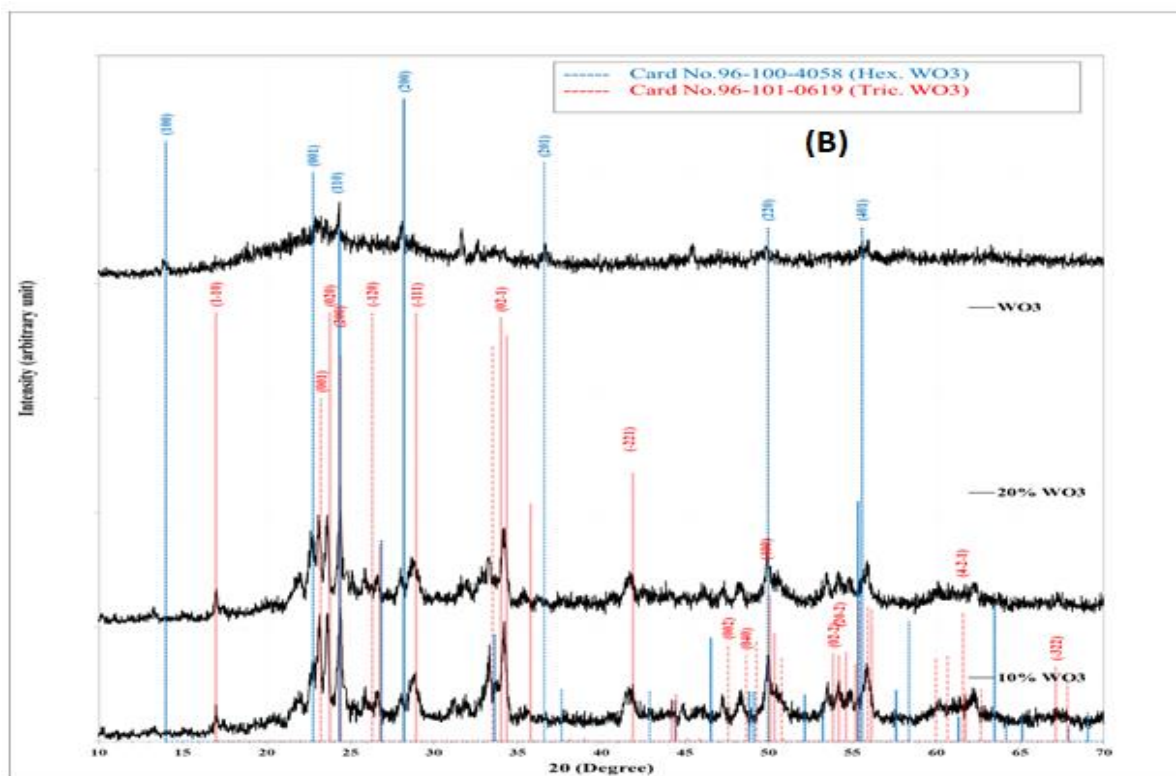


Figure 2-(A) X-ray diffraction pattern of pure PPy, (B) X-ray diffraction pattern of PPY:WO₃ (90:10% and 80:20%) hybrid nanocomposites.

3.2 Fourier Transform Infrared analyzes

The chemical composition of pure PPy and PPy–WO₃ nanocompounds was examined by FTIR spectrometry in the scope of 400–4000 cm⁻¹, as illustrated in Fig. 3. A characteristic peak at 786 cm⁻¹ is assigned to the C-H vibration, which shows deformation of planes at 1039 cm⁻¹. The peak at 1116 cm⁻¹ is ascribed to C-H inside and outside the planes deformation. The N-C stretch band and the C-H located inside the planes vibration are observed at 1209 cm⁻¹ and 1290 cm⁻¹, respectively. The C-C asymmetric wave extension and the stretching modes for the pyrrole ring are seen at 1467 cm⁻¹ and 1533 cm⁻¹, respectively [18-19]. Figure 3 displays the large frequency band at 700 cm⁻¹ as compared to the W-O-W stretch vibrations of the crystallized WO₃. The conspicuous spikes at 1633 cm⁻¹ might be because of the O-H vibrations. The spike at 3014 cm⁻¹ indicates an -OH assembly of tungsten oxide [19]. The results indicate that the WO₃ nanoparticles have a well crystalline structure when calcinated at 400 °C. The FTIR spectra of PPy–WO₃ (10% and 20%) hybrid nanocomposite show that the spikes at 3134 and 2997 cm⁻¹ are linked to C-H vibration stretching. The bending movement of the N-H appears at 1753 cm⁻¹. The PPy ring-extending and conjugated C-N wave extending bands appear at 1533 and 1467 cm⁻¹, respectively. The spikes at 1209 and 1039 cm⁻¹ are because of the C-N stretch and C-H distortion vibrations of PPy, respectively. Moreover, the spikes at 902 and 786 cm⁻¹ are identified with vibrations of N-H and C-H. It is clear from the figure below that the PPy–WO₃ hybrid nanocomposites show a shift in the peak positions of the main IR peaks. This indicates the occurrence of strain onto the molecules, i.e. obtaining new phase arrangement between PPy and WO₃ conformation. The FTIR results affirm the formation of the PPy–WO₃ hybrid nanocomposite.

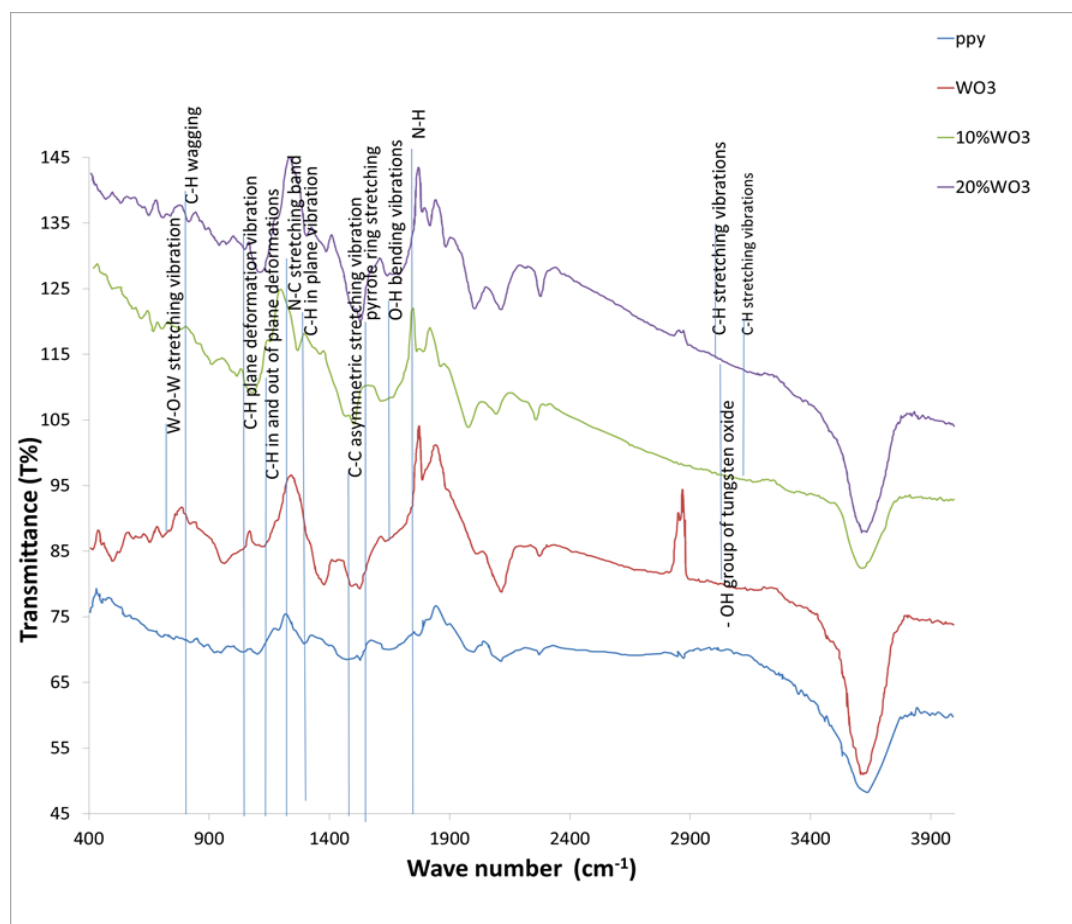


Figure 3-FTIR spectra of PPY, WO₃, and PPY-WO₃ (10:90% and 20:80%) hybrid nanocomposite.

3.3 Figure of merit of supercapacitor

3.3.1 Cyclic voltammetry

The results of cyclic voltammetry analysis of PPy and PPy-WO₃ films are portrayed in Fig. 4 (A–C). By repeating the scan rate (50, 70, 100) mV several times, we notice the clear peaks of the anode and cathode at (3.47, 3.54, 5.27), (3.41, 5.89, 8.82), and (6.96, 8.92, 12.5) mA, respectively. CV outcomes showed that the materials are electrochemically dynamic in the potential window. The PPy-WO₃ mixture film incorporates the electrochemical activities of both PPy and WO₃. As observed by figure 4, the nano WO₃-PPy membrane shows an observable electrochemical response below a positive potential of 0.3 V. The cathode electrode will be the charge storage for positive charge carriers inside the WO₃, while the anode electrode will be the positive charge emitter. This mechanism takes place during the discharge process. During the forms of CVs, the cathode side becomes black while the anode becomes white. The Gaussian shape in figure 4 reveals that the electrochemical interaction has a great significance in PPy-WO₃ composites, in contrast to pure PPy or WO₃. This could be well clarified using the synergistic impact of PPy and WO₃. In each curve in figure 4(A-C), the two strong redox peaks indicate a supercapacitor pseudo-capacitive property due to the reactions to the Faradaic redox [20]. Similar behavior was reported for the polyaniline-WO₃ composite membrane [20].

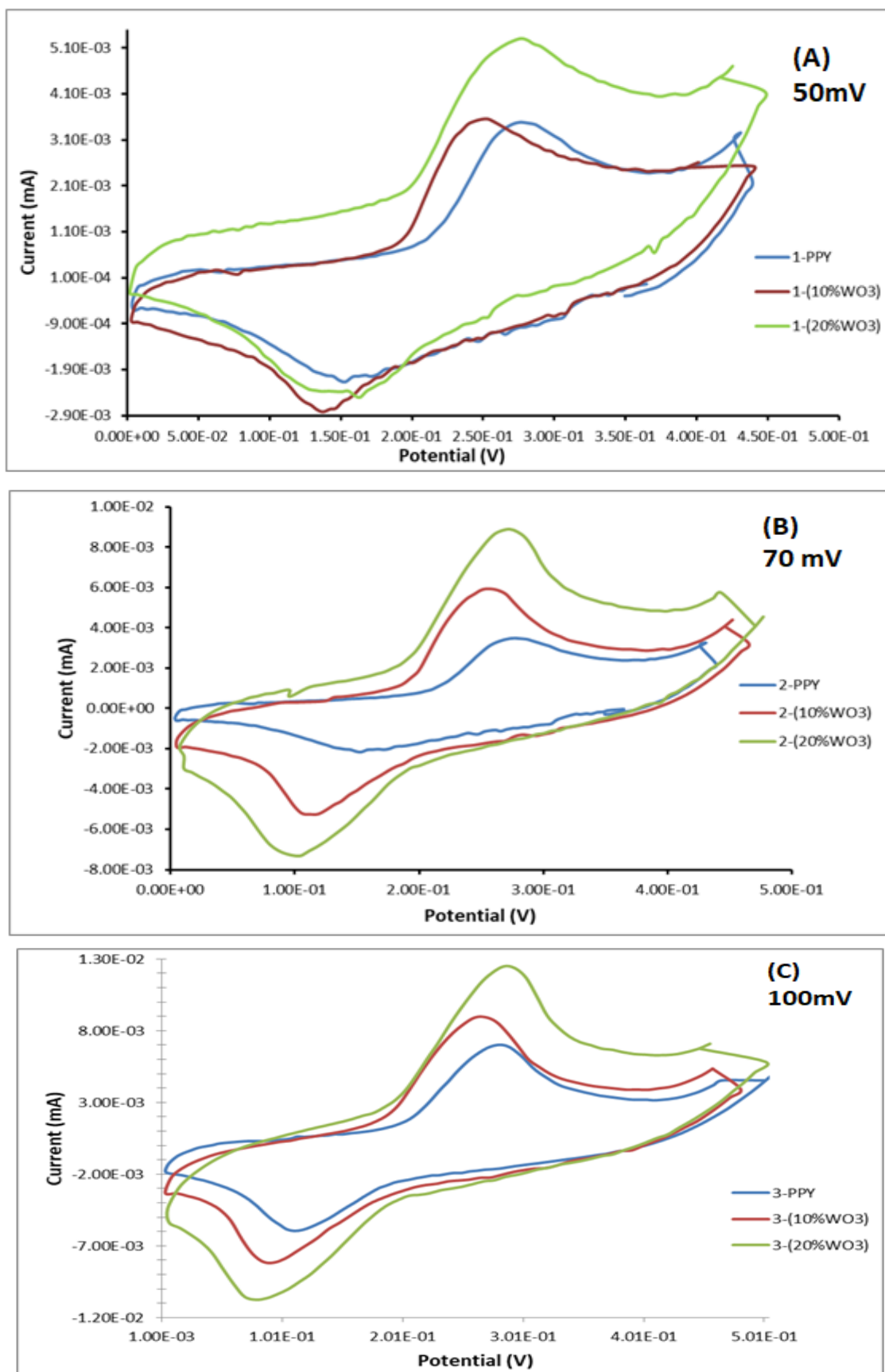


Figure 4 C-Cyclic voltammetry of PPY and PPY-WO₃ nanocomposite with different WO₃ concentrations at (A) 50mV, (B) 70mV, and (C) 100 mV

3.3-2 The stability of Cyclic voltammetry

The long-term cycle stabilization of PPy and PPy-WO₃ was evaluated by setting the cyclic voltammetry to 300 cycles in 1M H₂SO₄, as an electro-chemical solution, at a velocity of 50 (mV.S⁻¹). The results of the specific capacity, which is determined by the cyclic voltammetry test, are demonstrated in figures 5A and 5B. PPy-WO₃ was shown to maintain 80% specific capacity after 300 cycles. However, the specific capacity was increased with the increase in cycle number through the charge/discharge operation. The contact molecular collaboration between the WO₃ and PPy nanostructures confines the differences in the normal system frame through the charge/discharge process and improves the cycle stabilization of PPy-WO₃. The all-encompassing system frame is likewise liable for improved cycle stabilization of PPy-WO₃ [21]. The mass of the electrode of PPy or PPy-WO₃ is 0.7mg. The electrode stability can be calculated from the following equation [27]:

$$\text{Stability} = (C_n/C_1) \times 100$$

where C_n is the capacitance of the electrode in each cycle and C₁ is the capacitance of the first cycle. We found that the capacity of the pure PPy is (160, 215, 175, 181) F.g⁻¹. However, by adding 10% vol. of WO₃ to the PPy, we obtained a capacity of (166, 240, 209,213) F.g⁻¹, while when the ratio was increased to 20%, we recorded a capacity of (236, 266, 262,262) F.g⁻¹.

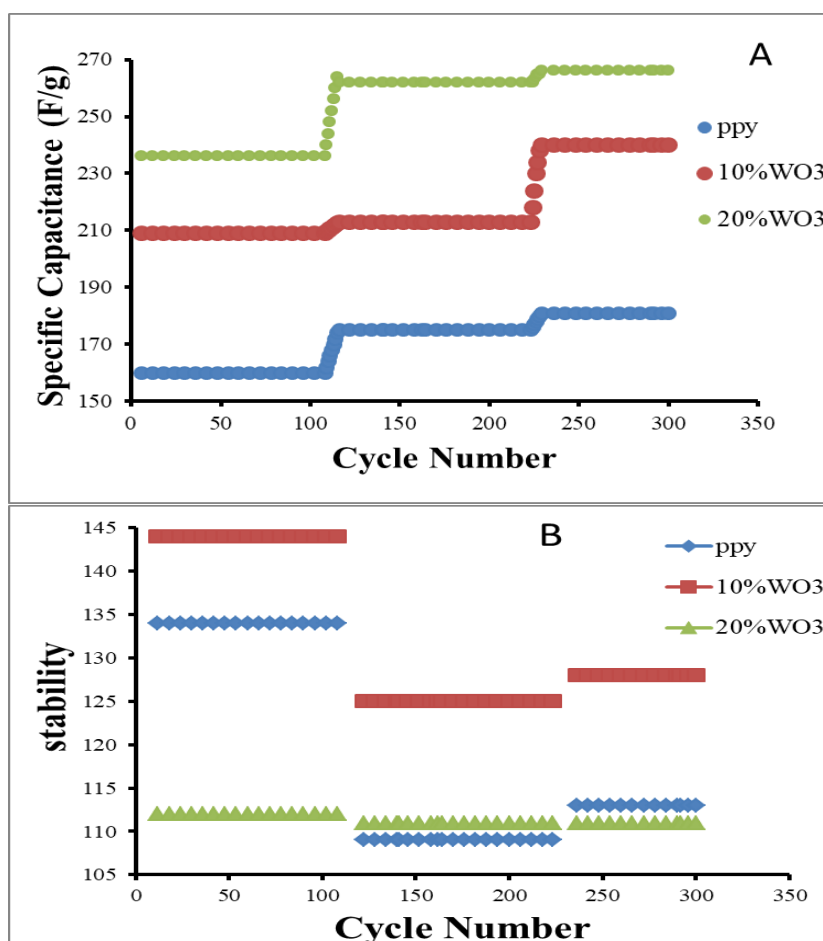


Figure 5 (A) Variation of specific capacitances with the change in cycle number of PPy and PPy-WO₃ nanocomposite in 1 M H₂SO₄ solution. (B) Variation of stability with the change in cycle number of PPy and PPy-WO₃ nanocomposite.

3.5 Galvanostatic charge and discharge examination

The electrochemical performance of the hybrid PPy-WO₃ electrode was conducted using galvanostatic charge / discharge test. Potential varieties for single electrodes were reported separately when a Ni-foam reference anode is added to ensure that the hybrid system will operate at the most notable work potential window. The potential varieties are practically slanting with one and two stages for the

negative and positive electrodes (presence of protrusions in the case of charging and discharging), respectively, which concur with the CV results shown in Fig.4. This is credited to the potential-subordinate nature of redox responses. The PPy is a p-doped (anion- inserting) polymer. This endless supply of the electrons from an unbiased fragment of their quinoid chains leads to some local positive charge distortion, making a polaron. In the event that the oxidation procedure proceeds further, more electrons must be expelled from the electrodes, bringing about the development of cation radicals, or bipolarons, which are vigorously liked to the arrangement of two separate polarons. In the event that the weight proportion PPy-WO₃ is not actually tuned, during the charging procedure, the oxidation and reduction of the WO₃ and the PPy electrodes, respectively, would not be complete, and the hybrid framework would work at a lower working potential window than anticipated [22, 24]. Nonetheless, during the charge/discharge forms (Fig. 6), both the PPy and the PPy-WO₃ electrodes work sensibly over the normal potential extents. Also, the hybrid composite PPy-WO₃ electrode can work at the working potential window 0.3V. The specific capacitance can be calculated from the CD curve using the following equation [23]

$$C = I \cdot \Delta t / \Delta V \cdot m$$

where C (F.g⁻¹) is specific capacitance, ΔV (V) is potential window (here 0.3V), I (A) is discharge current (here 8 mA), Δt (s) is discharge time (4.22 s for pure PPy, 6.2 s for 10% vol. of WO₃, 7 s for 20% vol. of WO₃), and m (g) is the mass of the electrode (PPY or PPy-WO₃, here 0.7mg) [24]. We obtained a capacity of pure PPy of 160 (F.g⁻¹) and, by adding 10% vol. of WO₃ to the PPy, we obtained a capacity of 240(F.g⁻¹), whereas when adding a quantity of up to 20% vol. of WO₃, we reached a capacity of 266.62 (F.g⁻¹). This might be due to the attraction between the tungsten oxide and polypyrrol nanoparticles, which leads to an increase in the surface area and, consequently, to an increase in the capacitance. The maximum value of the capacity was 266.6 (F/g), which it was obtained in 1 M H₂SO₄ electrolysis [13] and PPy plate -WO₃ nanocomposites by the oxidative polymerization technique.

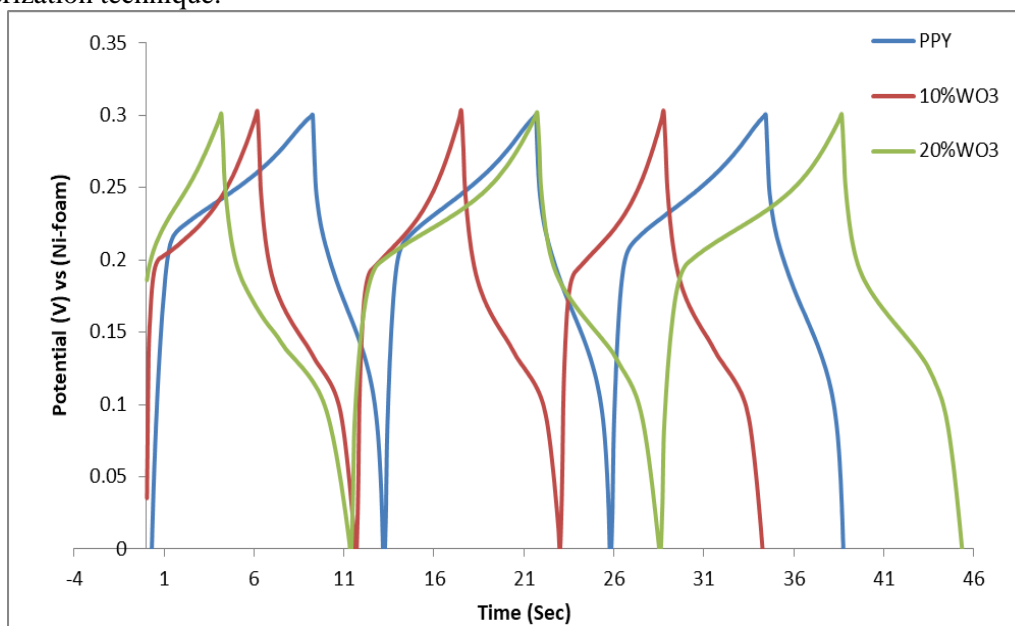


Figure 6-Galvanostatic charge–discharge results of PPy and PPy-WO₃ hybrid composite.

3.6 Electrochemical impedance spectroscopy measurements

Figure 7 displays the subsequent Nyquist EIS spectrum plots for the PPy, WO₃, and PPy-WO₃ complex anodes. A total spectrum made out of a high frequency arc was running and rising in the weak frequency extension. The arc on the real axis at high frequency indicates the equal series impedance. It is identified with the impedance of the electrical chemical solution, the total impedance of the internal and interfacial touch resistance of the electrolyte, the surface substance, and the current collector. The arc width is connected to the anode's load-transfer resistance (R_{ct}). This proposes that the simultaneous arrangement of a PPy-WO₃ covering has a contrast between the synergistic effect of both PPy and WO₃ and that of the individual segments alone. The decreased

resistance of the PPy-WO₃ terminal additionally shows a quicker Faradaic response, which is answerable for increased performance quality. Furthermore, at low frequencies, the PPy-WO₃ anode has a more perpendicular form than that of the pure PPy and pure WO₃, with good capacitive conduct and decreased diffusion impedance [25, 26].

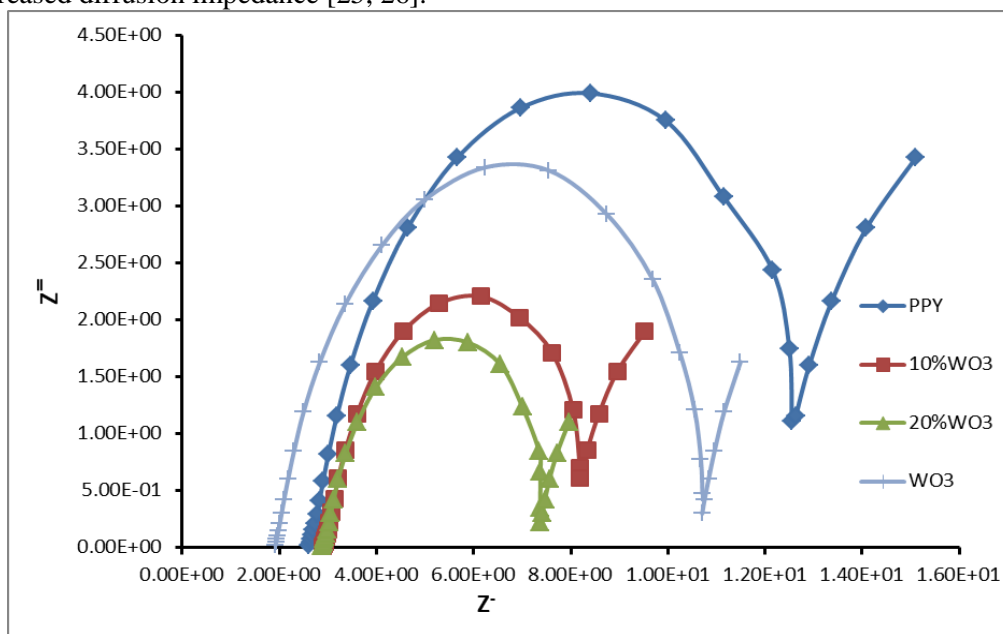


Figure 7 Nyquist plots of the electrochemical impedance spectroscopy for the PPy, WO₃ and PPy-WO₃ hybrid composite electrodes.

Conclusions

The PPy-WO₃ nanocomposites were prepared successfully by a simple oxidative method. The PPy-WO₃ nanocomposite has a higher electrochemical movement than that of the pure PPy or WO₃. The highest cyclic voltammetry stability of PPy-WO₃ was at 20% of WO₃, where a large specific capacity of 266.62 (F.g⁻¹) was estimated. This capacitance percentage is greater than that of the pure PPy 215 (F.g⁻¹). At low frequencies, the PPy-WO₃ anode has a more perpendicular form as compared to that of the pure PPy and pure WO₃.

References

1. K. Dutta, S. Das, D. Rana, and P. P. Kundu, "Enhancements of catalyst distribution and functioning upon utilization of conducting polymers as supporting matrices in DMFCs: a review," *Polym. Rev.*, vol. 55, no. 1, pp. 1–56, 2015.
2. P. Santhosh, A. Gopalan, and K.-P. Lee, "Gold nanoparticles dispersed polyaniline grafted multiwall carbon nanotubes as newer electrocatalysts: preparation and performances for methanol oxidation," *J. Catal.*, vol. 238, no. 1, pp. 177–185, 2006.
3. J. Ding, K. Zhang, W. Xu, and Z. Su, "Self-assembly of gold nanoparticles on gold core-induced polypyrrole nanohybrids for electrochemical sensor of dopamine," *Nano*, vol. 10, no. 08, p. 1550115, 2015.
4. K. E. Hnida, R. P. Socha, and G. D. Sulka, "Polypyrrole–silver composite nanowire arrays by cathodic co-deposition and their electrochemical properties," *J. Phys. Chem. C*, vol. 117, no. 38, pp. 19382–19392, 2013.
5. Z. Huang, P.-C. Wang, A. G. MacDiarmid, Y. Xia, and G. Whitesides, "Selective deposition of conducting polymers on hydroxyl-terminated surfaces with printed monolayers of alkylsiloxanes as templates," *Langmuir*, vol. 13, no. 24, pp. 6480–6484, 1997.
6. J. Jang, "Conducting polymer nanomaterials and their applications," in *Emissive Materials Nanomaterials*, Springer, 2006, pp. 189–260.
7. A. Babakhanian, S. Kaki, M. Ahmadi, H. Ehzari, and A. Pashabadi, "Development of α -polyoxometalate–polypyrrole–Au nanoparticles modified sensor applied for detection of folic acid," *Biosens. Bioelectron.*, vol. 60, pp. 185–190, 2014.

8. P. Novák, K. Müller, K. S. V Santhanam, and O. Haas, "Electrochemically active polymers for rechargeable batteries," *Chem. Rev.*, vol. 97, no. 1, pp. 207–282, 1997.
9. X. Lu *et al.*, "A novel nanocomposites sensor for epinephrine detection in the presence of uric acids and ascorbic acids," *Electrochim. Acta*, vol. 56, no. 21, pp. 7261–7266, 2011.
10. Y.-Z. Long *et al.*, "Recent advances in synthesis, physical properties and applications of conducting polymer nanotubes and nanofibers," *Prog. Polym. Sci.*, vol. 36, no. 10, pp. 1415–1442, 2011.
11. Q. Zhang, X. Zhou, and H. Yang, "Capacitance properties of composite electrodes prepared by electrochemical polymerization of pyrrole on carbon foam in aqueous solution," *J. Power Sources*, vol. 125, no. 1, pp. 141–147, 2004.
12. H. Kang and K. E. Geckeler, "Enhanced electrical conductivity of polypyrrole prepared by chemical oxidative polymerization: effect of the preparation technique and polymer additive," *Polymer (Guildf.)*, vol. 41, no. 18, pp. 6931–6934, 2000.
13. H. An *et al.*, "Polypyrrole/carbon aerogel composite materials for supercapacitor," *J. Power Sources*, vol. 195, no. 19, pp. 6964–6969, 2010.
14. X. Yang and L. Li, "Polypyrrole nanofibers synthesized via reactive template approach and their NH₃ gas sensitivity," *Synth. Met.*, vol. 160, no. 11–12, pp. 1365–1367, 2010.
15. B. T. Raut, M. A. Chougule, A. A. Ghanwat, R. C. Pawar, C. S. Lee, and V. B. Patil, "Polyaniline–CdS nanocomposites: effect of camphor sulfonic acid doping on structural, microstructural, optical and electrical properties," *J. Mater. Sci. Mater. Electron.*, vol. 23, no. 12, pp. 2104–2109, 2012.
16. G. D. Khuspe *et al.*, "Facile method of synthesis of polyaniline–SnO₂ hybrid nanocomposites: Microstructural, optical and electrical transport properties," *Synth. Met.*, vol. 178, pp. 1–9, 2013.
17. M. Thakurdesai, N. Kulkarni, B. Chalke, and A. Mahadkar, "Synthesis of CdSe films by a annealing of Cd/Se bilayer" *Chalcogenide Lett.*, vol. 8, no. 3, pp. 223–229, 2011.
18. A. Batool, F. Kanwal, M. Imran, T. Jamil, and S. A. Siddiqi, "Synthesis of polypyrrole/zinc oxide composites and study of their structural, thermal and electrical properties," *Synth. Met.*, vol. 161, no. 23–24, pp. 2753–2758, 2012.
19. A. T. Mane, S. T. Navale, S. Sen, D. K. Aswal, S. K. Gupta, and V. B. Patil, "Nitrogen dioxide (NO₂) sensing performance of p-polypyrrole/n-tungsten oxide hybrid nanocomposites at room temperature," *Org. Electron.*, vol. 16, pp. 195–204, 2015.
20. C. Dulgerbaki and A. U. Oksuz, "Fabricating polypyrrole/tungsten oxide hybrid based electrochromic devices using different ionic liquids," *Polym. Adv. Technol.*, vol. 27, no. 1, pp. 73–81, 2016.
21. S. Sahoo, S. Dhibar, G. Hatui, P. Bhattacharya, and C. K. Das, "Graphene/polypyrrole nanofiber nanocomposite as electrode material for electrochemical supercapacitor," *Polymer (Guildf.)*, vol. 54, no. 3, pp. 1033–1042, 2013.
22. J. Li and F. Gao, "Analysis of electrodes matching for asymmetric electrochemical capacitor," *J. Power Sources*, vol. 194, no. 2, pp. 1184–1193, 2009.
23. Y. Yan, H. Li, Y. Zhang, J. Kan, and T. Jiang, "Facile Synthesis of Polypyrrole Nanotubes and Their Supercapacitive Application," vol. 12, pp. 9320–9334, 2017, doi: 10.20964/2017.10.61.
24. H. R. Ghenaatian, M. F. Mousavi, and M. S. Rahmanifar, "High performance hybrid supercapacitor based on two nanostructured conducting polymers: Self-doped polyaniline and polypyrrole nanofibers," *Electrochim. Acta*, vol. 78, pp. 212–222, 2012, doi: 10.1016/j.electacta.2012.05.139.
25. L. Bao, J. Zang, and X. Li, "Flexible Zn₂SnO₄/MnO₂ core/shell nanocable– carbon microfiber hybrid composites for high-performance supercapacitor electrodes," *Nano Lett.*, vol. 11, no. 3, pp. 1215–1220, 2011.
26. J. G. Wang, Y. Yang, Z. H. Huang, and F. Kang, "Rational synthesis of MnO₂/conducting polypyrrole@carbon nanofiber triaxial nano-cables for high-performance supercapacitors," *J. Mater. Chem.*, vol. 22, no. 33, pp. 16943–16949, Sep. 2012, doi: 10.1039/c2jm33364c.
27. J. S. Shayeh, A. Ehsani, M. R. Ganjali, P. Norouzi, and B. Jaleh, "Conductive polymer/reduced graphene oxide/Au nano particles as efficient composite materials in electrochemical supercapacitors," *Appl. Surf. Sci.*, vol. 353, pp. 594–599, 2015